J|A|C|S
ARTICLES
Published on Web 09/10/2002

# The Repulsive Coulomb Barrier along a Dissociation Path of the $BeC_4^{2-}$ Dianion

Qicun Shi and Sabre Kais*

*Contribution from the Department of Chemistry, Purdue University, West Lafayette, Indiana 47907*

Received January 23, 2002. Revised Manuscript Received May 1, 2002

***Abstract:*** We present ab initio calculations of the repulsive Coulomb barrier for several geometrically stable isomers of the $BeC_4^{2-}$ dianion. We describe how the deformation of certain isomers can account for the experimental Coulomb explosion images of the dianion. For the most stable linear isomer, $C_2^-BeC_2^-$, we examined the electron tunneling process along the dissociation path to obtain $C_2^-$ plus $BeC_2^-$. We found the crossing point for autodetachment to be $R_{dis}^c = 3.25$ Å. $R_{dis}$ is the bond length between $C_2^-$ and $BeC_2^-$; at this point, the electron tunneling energy is equal to the maximum of the repulsive Coulomb barrier. In the framework of the Wenzel−Kramer−Brioullin theory, the electron-loss lifetime of the metastable $C_2^-BeC_2^-$ dianion at the equilibrium geometry, $R_{dis} = 1.64$ Å, was estimated to be about 5 ms. This lower limit is in agreement with the experimental results in which the $BeC_4^{2-}$ dianion has a lifetime much longer than 5 $\mu$s.

## I. Introduction

In recent years, there has been considerable interest in the formation and stability of gas-phase dianions.[1−10] A stable dianion has to possess two basic properties: First, it must be stable with respect to electron autoejection, and, second, it must be stable with respect to fragmentation of the nuclear framework. Dianions in the gas phase have been observed only recently, although they are common in condensed phases.[11] The strong Coulomb repulsion between the excess charges makes the dianions unstable relative to electron autoejection or fragmentation. However, the repulsive Coulomb barrier (RCB) provides dynamic stability.[7] For dianions, the RCB emerges as a result of combining the short-range binding energy of the excess electron and the long-range electrostatic repulsion between the outgoing electron and the anion. This RCB has to be passed by the outgoing electron during its detachment process which can render substantial lifetimes even for thermodynamically unstable dianions. The RCB is a general property of multiply charged anions.[2]

The RCB plays an important role in searching for long-lived gas-phase multiply charged ions, and it was examined with both experiment and theory. Experimentally, Compton et al.[1,8,12] have examined the RCB in the investigation of doubly charged fullerene dianions such as the metastable long-lived $C_{60}^{2-}$ and the highly fluorinated stable dianion $C_{60}F_{48}^{2-}$. Wang et al.[13−16] provided significant advances in the photoelectron experiments for studying multiply charged anions and gave direct experimental proof of the existence of the RCB for the dicarboxylate dianions $^-O_2C-(CH_2)_n-CO_2^-$ with $n = 2-6$, three isomers of the benzene dicarboxylate dianions, and other dianions. From the theoretical point of view, Cederbaum et al.[17] outlined a theoretical procedure relating the RCB to the theory of Green's functions and argued that the exact potential, which the electron experiences, is nonlocal and energy dependent. Because it is complicated to compute the nonlocal potential, they introduced an approximate local potential to calculate the RCB for dianions, including atomic dianions, $F^{2-}$ and $O^{2-}$, linear carbon clusters dianions $C_n^{2-}$ ($n = 2, 4, 6, 8$),[17] and mixed beryllium carbon dianions $BeC_n^{2-}$.[18] Simons et al.[2,19,20] demonstrated that a simple Coulomb-energy model can be used to predict the vertical electron detachment and to estimate the RCB for stable and metastable multiply charged anions such as $MgF_4^{2-}$, $BeF_4^{2-}$, and $SO_4^{2-}$.

* To whom correspondence should be addressed. E-mail: kais@power1.chem.purdue.edu.

(1) Scheller, M. K.; Compton, R. N.; Cederbaum, L. S. *Science* **1995**, *270*, 1160.
(2) Simons, J.; Skurski, P.; Barrios, R. *J. Am. Chem. Soc.* **2000**, *122*, 11893.
(3) Schauer, S. N.; Williams, P.; Compton, R. N. *Phys. Rev. Lett.* **1990**, *65*, 625.
(4) Dolgounitcheva, O.; Zakrzewski, V. G.; Ortiz, J. V. *J. Chem. Phys.* **1998**, *109*, 87.
(5) Watts, J. D.; Bartlett, R. *J. Chem. Phys.* **1992**, *97*, 3445.
(6) Lieb, E. H. *Phys. Rev. Lett.* **1984**, *52*, 315.
(7) Wang, X. B.; Wang, L. S. *Nature* **1999**, *400*, 245.
(8) Lin, C.; Hettich, R. L.; Compton, R. N.; Tuinman, A.; Derecskei-Kovacs, A.; Marynick, D. S.; Dunlap, B. I. *Phys. Rev. Lett.* **1994**, *73*, 2821.
(9) Klein, J.; Middleton, R. *Nucl. Instrum. Methods Phys. Res., Sect. B* **1999**, *159*, 8.
(10) Simons, J.; Jordan, K. D. *Chem. Rev.* **1987**, *87*, 535.
(11) Dougherty, R. C. *J. Chem. Phys.*, **1969**, *50*, 1896.
(12) Compton, R. N.; Tuinman, A.; Klots, C. E.; Pederson, M. R.; Patton, D. C. *Phys. Rev. Lett.* **1997**, *78*, 4367.
(13) Wang, X. B.; Nicholas, J. B.; Wang, L. S. *J. Chem. Phys.* **2000**, *113*, 653.
(14) Wang, X. B.; Wang, L. S. *J. Phys. Chem.* **2000**, *104*, 4429.
(15) Wang, X. B.; Wang, L. S. *J. Am. Chem. Soc.* **2000**, *122*, 2339.
(16) Wang, X. B.; Wang, L. S. *J. Chem. Phys.* **1999**, *111*, 4497.
(17) Dreuw, A.; Cederbaum, L. S. *Phys. Rev. A* **2001**, *63*, 049904-1.
(18) Dreuw, A.; Cederbaum, L. S. *J. Chem. Phys.* **2000**, *112*, 7400.
(19) Skurski, P.; Simons, J.; Wang, X. B.; Wang, L. S. *J. Am. Chem. Soc.* **2000**, *122*, 4499.
(20) Boldyrev, A. I.; Simons, J. *J. Chem. Phys.* **1993**, *98*, 4745.

***Table 1.*** Energies (au) from Hartree−Fock (HF) and Configuration Interaction with Single Plus Double Excitations (CISD) for Different Basis Sets for the Symmetrical Nuclear Configuration of the Linear Isomer A

| | HF | | | | CISD | | |
|---|---|---|---|---|---|---|---|
| molecules | D95+(d) | DZP[a] | 6-311+G(d) | DZ[18] | D95+(d) | DZP[a] | 6-311+G(d) |
| $BeC_4$ | −165.5973 | −165.6035 | −165.6058 | | −166.3151 | −166.3225 | −166.3435 |
| $BeC_4^{1-}$ | −165.8955 | −165.9017 | −165.9048 | | −166.4569 | −166.4640 | −166.4877 |
| $BeC_4^{2-}$ | −165.9037 | −165.9098 | −165.9136 | 165.9074 | −166.4563 | −166.4635 | −166.4897 |

[a] We used the reoptimized (9s/5p)/[4s2p] contracted-Gaussian-type-function basis sets[21] plus a d-polarization function with exponent from Dunning and Hay.[22]

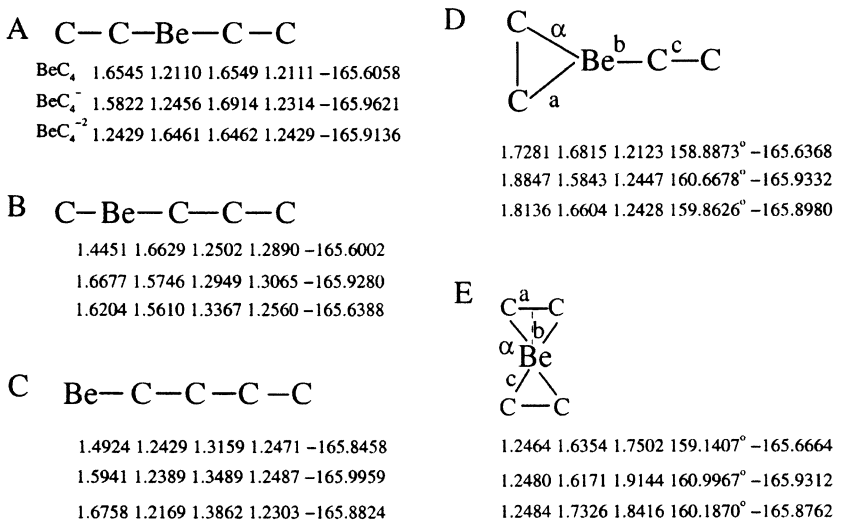


***Figure 1.*** Several possible equilibrium geometries of the $BeC_4^{2-}$ dianion, three linear structures (A, B, C) and two planar structures (D, E). The optimized distances (in Å) and energies (in atomic units) at the Hartree−Fock level of theory are given for $BeC_4$, $BeC_4^{1-}$, and $BeC_4^{2-}$. The geometric parameters and energy are represented in the form ($a$, $b$, ...; $\alpha$, $\beta$, ...; $\phi_1$, $\phi_2$, ...; energy), where $a$, $b$, ... are bond lengths in Å, $\alpha$, $\beta$, ... (in deg) are the bond angles, and $\phi_1$, $\phi_2$, ... (in deg) are dihedral angles followed by the energy in atomic units.

In this paper, we examine the variation of the RCB along the dissociation path for $BeC_4^{2-}$. This dianion was observed experimentally in a mass spectrometer by Klein and Middleton.[9]

Klein and Middleton[9] attempted to determine the molecular structure of the $BeC_n^{2-}$ ions from Coulomb explosion images. Although these images present convincing support for the identification of the dianions, they make it clear how difficult it is to extract structural information from the images. They proposed two possible structures for $BeC_n^{2-}$: one is linear and rigid with the Be atom located at the terminus of the carbon chain, while the other structure consists of two rigid linear carbon chains joined at an angle >100° with the Be atom at the joining point. They also stress the fact that the Coulomb explosion images provide little evidence in favor of one structure over the other. Dreuw and Cederbaum[18] examined in detail, using ab initio methods, several possible structures for $BeC_4^{2-}$ and investigated their stability with respect to electron autodetachment as well as with respect to fragmentation. They have found that only linear isomers represent geometrically stable isomers, but it is not clear how the isomers relate to the Coulomb explosion images. In the present work, we first confirm the results of Dreuw and Cederbaum, and in section II we show how the Coulomb explosion images might be related to our optimized structures.

In section III, we considered the electron detachment during vibrational motion of the dianion $BeC_4^{2-}$. We investigated all possible fragmentation channels. We also examined the electron tunneling process along the dissociation path to obtain $C_2^-$ plus $BeC_2^-$. We have found the crossing point for autodetachment to be $R_{dis}^c = 3.25$ Å; $R_{dis}$ is the bond length between $C_2^-$ and Be $C_2^-$. At this point, the electron tunneling energy is equal to the maximum of the repulsive Coulomb barrier. Finally, we examined how the tunneling varies along the dissociation path in two directions $Y$ and $Z$ in the molecular plane using the Wenzel−Kramer−Brioullin (WKB) theory.

## II. Geometry Optimization

All of the molecular geometries of $BeC_4$ isomers were optimized at the Hartree−Fock (HF) level of theory with 6-311+G(d) basis set; this basis set seems sufficient to describe the characteristics of the examined isomers of $BeC_4$ (see Table 1), followed by the vibrational analysis that is used to check for possible imaginary values. The effect of electron correlation on the energetics of the optimized geometries was studied by calculations with the second-order perturbation theory (MP2) as well as configuration interaction with single plus double excitations (CISD).

To obtain the possible molecular structures for $BeC_4^{2-}$, we considered various initial nuclear geometric structures, including linear, cyclic, and three-dimensional isomers. Only structures for which the energy of the dianion is lower than that of the neutral molecule are shown in Figure 1. These isomers labeled by A, B, C, D, and E are planar, and all represent minima on the $BeC_4^{2-}$ potential energy surface. The geometric parameters and energy of each isomer are given in Figure 1.

Among all of the possible isomers, we have found, using HF and CISD, that isomer A in Figure 1 has the lowest dianion energy. This finding is consistent with the previous work of

Dreuw and Cederbaum[18] in which they reported that the strictly linear isomer consists of a central Be atom to which two electron affine acetylid groups are bound with $D_{\infty h}$ symmetry, which represents a minimum on the potential energy surface and is stable with respect to electron autoejection at the level of Koopmans' theorem.[18]

The ground state of isomer A is a closed-shell $^1\Sigma_g^+$ state. To examine the effect of different basis sets on the calculated energies, we compared the HF and CISD results using double-$\zeta$ (DZ) basis sets[18,21,22] and the intrinsic basis sets in the Gaussian 98 package,[23] D95, 6-31G, and 6-311G, as well as additions of d-type polarizations and (s,p)-type diffuse functions. Because the effect of different basis sets on our results is small as shown in Table 1, it seems that 6-311G basis set plus a d-type polarization function and a single additional diffuse s and p function, that is, 6-311+G(d), is ideal for this system and will be used in all of our calculations on $BeC_4^{2-}$ dianions.

After geometry optimizations, we further examined isomers A, D, and E without symmetry constraints. This step is very important for the anion because of the odd number of electrons. Hence, we have only two choices for the electron density distribution: symmetrical and nonsymmetrical. We first examined the nonsymmetrical variables for the C−C−Be−C−C molecule. Because each bond length is about 1.2−1.5 Å, the linear system extends about 5 Å along the molecular axis, while its vertical extent is on the order of an atomic size (C, Be), ∼1 Å. For the anion, the excess electron will not occupy such an elongated (5 Å) molecular orbital. For the dianion, we have an even number of electrons, and the electron density should be symmetrical with an extended density of about one-half the molecular length (∼2 Å). The bond between $C_2$ and Be is similar to the bond of a diatomic molecule ($C_2$−Be−$C_2$). From this analysis, we conclude that for anions with one excess electron, the electron density must be nonsymmetrical, thus leading to a situation where the electron is localized on one side of the linear anion which is of a lower energy as compared with the symmetrical one. In Figure 2, we use the Mulliken charges to show the electron localization in the anion $BeC_4^-$. The height of each column in the histograms equals the Mulliken charges on each atom. Dashed lines correspond to the symmetrical structures, and solid lines correspond to the nonsymmetrical structures.

Klein and Middleton[9] attempted to determine the molecular structure of the $BeC_n^{2-}$ ions from Coulomb explosion images. Although these images present convincing support for the identification of the dianions, they make it clear how difficult it is to extract structural information from them. To understand these Coulomb explosion images and how they might be related

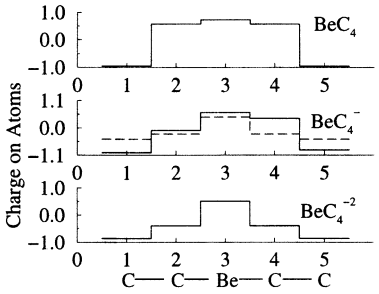


***Figure 2.*** Mulliken charges for $BeC_4$, $BeC_4^-$, and $BeC_4^{2-}$. Solid lines correspond to the optimized set of symmetrical variables, while the dashed lines correspond to the nonsymmetrical variables.

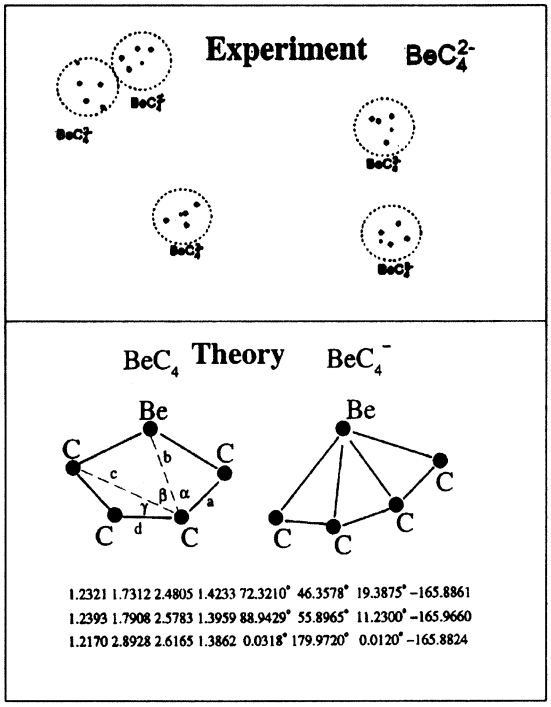


***Figure 3.*** The top insert is the experimental Coulomb explosion images for the $BeC_4^{2-}$ dianion (taken from the work of Klein and Middleton[9]). The bottom insert has the HF results of a planar isomer which has an energy lower than isomer A and close to that of the linear isomer C. Also included at the bottom of the figure are the optimized parameters for $BeC_4$, $BeC_4^{1-}$, and $BeC_4^{2-}$ (note that the parameters for $BeC_4^{2-}$ are very close to that of isomer C; the structure is not shown).

to our optimized structures in Figure 1, we compare optimized structures at the HF level with the experimental Coulomb explosion images[9] as shown in Figure 3. In that figure, we show that the optimized structures for $BeC_4$ and $BeC_4^-$ are planar, but for the $BeC_4^{2-}$ dianion it is similar to isomer C in Figure 1. The planar anion has an HF energy of −165.9660 au (see Table 2 for comparison), which is lower than the anionic energy of the chain structure A (−165.9621 au) and is close to the lowest energy of the chain structure C (−165.9959 au). Because the energies of isomers C, D, and E of the dianion are very close, one can consider the possible motions of the tight C−C bonds relative to the Be atom to form the most stable isomer A. Thus, the intermediate images of the planar structures are consistent with our optimized structures. This might support a shake-off mechanism in which one or two excess electrons are shaken off the dianion just before the Coulomb explosion happens.[24]

(21) Thakkar, A. T.; Koga, T.; Saito, M.; Hoffmeyer, R. E. *Int. J. Quantum Chem.* **1993**, *27*, 343 and references therein.
(22) Dunning, T. H., Jr.; Hay, P. J. In *Methods of Electronic Theory*; Schaefer, H. F., III, Ed.; Plenum Press: New York, 1977.
(23) Frisch, M. J.; Trucks, G. W.; Schlegel, H. B.; Scuseria, G. E.; Robb, M. A.; Cheeseman, J. R.; Zakrzewski, V. G.; Montgomery, J. A., Jr.; Stratmann, R. E.; Burant, J. C.; Dapprich, S.; Millam, J. M.; Daniels, A. D.; Kudin, K. N.; Strain, M. C.; Farkas, O.; Tomasi, J.; Barone, V.; Cossi, M.; Cammi, R.; Mennucci, B.; Pomelli, C.; Adamo, C.; Clifford, S.; Ochterski, J.; Petersson, G. A.; Ayala, P. Y.; Cui, Q.; Morokuma, K.; Malick, D. K.; Rabuck, A. D.; Raghavachari, K.; Foresman, J. B.; Cioslowski, J.; Ortiz, J. V.; Baboul, A. G.; Stefanov, B. B.; Liu, G.; Liashenko, A.; Piskorz, P.; Komaromi, I.; Gomperts, R.; Martin, R. L.; Fox, D. J.; Keith, T.; Al-Laham, M. A.; Peng, C. Y.; Nanayakkara, A.; Gonzalez, C.; Challacombe, M.; Gill, P. M. W.; Johnson, B.; Chen, W.; Wong, M. W.; Andres, J. L.; Gonzalez, C.; Head-Gordon, M.; Replogle, E. S.; Pople, J. A. *Gaussian 98*, revision A.7; Gaussian, Inc.: Pittsburgh, PA, 1998.
(24) Klein, J.; Middleton, R. *Phys. Rev. A* **1999**, *60*, 3515.

***Table 2.*** Hartree−Fock (HF) Energies (au) for Isomers A, B, C, D, E as Shown in Figure 1 and the Intermediate (I) Structures as Shown in Figure 3 for the Molecule, Anion, and Dianion[a]

| | A | B | C | D | E | I |
|---|---|---|---|---|---|---|
| $BeC_4$ | −165.6058 | −165.6002 | −165.8458 | −165.6368 | −165.6664 | −165.8861 |
| $BeC_4^{1-}$ | −165.9621 | −165.9280 | −165.9959 | −165.9332 | −165.9312 | −165.9660 |
| | −0.3563 | −0.3278 | −0.1501 | −0.2964 | −0.2648 | −0.0799 |
| $BeC_4^{2-}$ | −165.9136 | −165.6388 | −165.8824 | −165.8980 | −165.8762 | −165.8824 |
| | 0.0485 | 0.2892 | 0.1135 | 0.0352 | 0.0550 | 0.0836 |

[a] There are two values for each entry, the upper one being the total energy, and the lower one is the relative value. The relative value is the difference between the dianion and the anion and between the anion and the molecule.

There is then a certain period of relaxation during which the linear structure transfers into a planar structure.

### III. The Repulsive Coulomb Barrier along the Dissociation Path

Simons[25,26] has shown that molecular anions possessing excess internal vibrational or rotational energy can lose their extra electron through radiationless transitions involving non-Born−Oppenheimer coupling. The same could happen for dianions; one of the excess electrons can detach during vibrational or rotational motion along the potential energy surface. Here we consider the electron detachment during vibrational motion of the dianion $BeC_4^{2-}$. First, let us consider all possible fragmentation channels. Fragmentation of the dianion into two monoanionic fragments is favorable due to the strong electrostatic repulsion; thus channels with two charged products are

$$BeC_4^{2-} \rightarrow Be^- + C_4^- \quad (1)$$

$$BeC_4^{2-} \rightarrow BeC^- + C_3^- \quad (2)$$

$$BeC_4^{2-} \rightarrow BeC_2^- + C_2^- \quad (3)$$

$$BeC_4^{2-} \rightarrow BeC_3^- + C \quad (4)$$

$$BeC_4^{2-} \rightarrow BeC_4^- + e^- \quad (5)$$

From our calculations of the different channels, we found that channel 3 is the energetically favored fragmentation channel because it has the lowest dissociation threshold at −165.8410 au. This is lower than the second dissociation threshold from the channel, $Be^- + C_4^-$, by 1.3 eV. In addition, channel 1 is not available because the EA of Be is negative.[27] This finding is in full agreement with the previous conclusion[18] that the dianion $BeC_4^{2-}$ has a stable structure consisting of a central Be atom to which two electron affine acetylid groups are bound with a Be−C single bond and the C−C triple bond.

In our HF and CISD calculations, we chose the dissociation path along the principal molecular axis, which is the linear axis for structures A, B, C, D, and E. HF and CISD methods we applied might not be the best methods to investigate "weakly bound" systems and fragmentation (CISD is also not size-consistent). Yet, our CISD and MP2 results for the optimized energies at the equilibrium for $C_2BeC_2^{2-}$ were in complete agreement with the CCSD results. Figure 4 shows the calculated

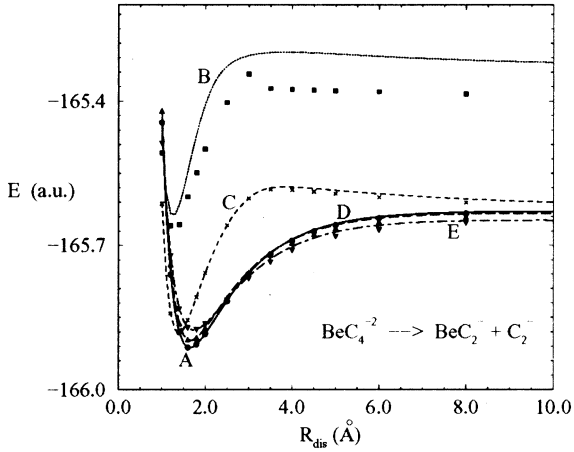


***Figure 4.*** Molecular potential energy curves for the five geometric configurations of $BeC_4^{2-}$ as a function of the distance between the two fragments $C_2^-$ and $BeC_2^-$ ($R_{dis}$). Full dots represent the energies of the reoptimized structures at a given $R_{dis}$, and the curves correspond to equilibrium energies of different structures where only $R_{dis}$ varies.

molecular potential energy as a function of $R_{dis}$, which is the separation distance (bond length) between $C_2$ and $BeC_2$. In Figure 4, we compare two types of calculations; dots represent the energies of the reoptimized structures at a given $R_{dis}$, and the curves correspond to equilibrium energies of different structures where only $R_{dis}$ varies. It is clear from the figure that the dissociation path is along the principal molecular axis for structures A, C, D, and E.

The strong Coulomb repulsion between the excess charges makes the dianions unstable relative to electron autodetachment or fragmentation. However, the RCB provides dynamic stability. For dianions, the RCB emerges as a result of combining the short-range binding energy of the excess electron and the long-range electrostatic repulsion between the outgoing electron and the anion. This Coulomb barrier has to be passed by the outgoing electron. This barrier has been discussed by several groups: Compton et al.,[8] Wang et al.,[13] Simons,[2] and Dreuw and Cederbaum.[18]

Cederbaum and co-workers have discussed the complexity of the exact calculations of the Coulomb barrier, which is a nonlocal and energy-dependent potential.[17] In principle, it can be obtained using Green's function methods, but in practice it is not straightforward to compute it. To approximate the repulsive Coulomb barrier, we first follow the approximation developed by Dreuw and Cederbaum,[18] the frozen orbital static approximation. In this approximation, one takes out one electron from the highest occupied molecular orbital of the dianion, which is the orbital from which the electron is detached. One then calculates the electrostatic potential by summing up the

(25) Simons, J. *J. Am. Chem. Soc.* **1981**, *103*, 3971.
(26) Simons, J. *J. Phys. Chem.* **1999**, *103*, 9408.
(27) Kvale, T. J.; Alton, G. D.; Compton, R. N.; Pegg, D. J.; Thompson, J. S. *Phys. Rev. Lett.* **1985**, *55*, 484.

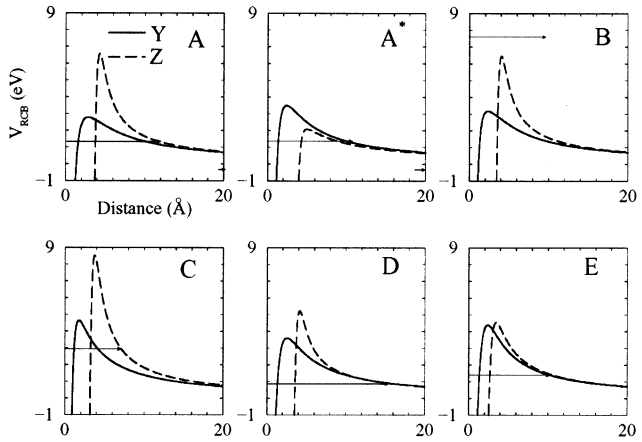


***Figure 5.*** One-dimensional Hartree−Fock repulsive Coulomb barrier curves along the molecular axis $\hat{Z}$ (thick dashed lines) and its vertical axis $\hat{Y}$ (thick solid lines) for the five equilibrium geometries A, B, C, D, and E of the Be $C_4^{2-}$ dianion. The curves are obtained from the molecular electrostatic potential with frozen orbitals of $BeC_4^{2-}$ dianions as one of the electrons in the highest occupied molecular orbital (HOMO) tunnels out. Insert A* indicates the correct Coulomb potential limit of electron detachment of dianion $BeC_4^{2-}$, which is calculated with the frozen orbitals of the $BeC_4^{1-}$ anion interacting with a negative point charge. The tunneling energy (thin solid line) is assumed to be the negative value of the vertical (shown here) or the adiabatic (not shown here) electron detachment energy.

electron−nucleus attractions and the electron−electron repulsions

$$V(r) = -\sum_{\alpha=1}^{K} \frac{Z_\alpha}{|r - r_\alpha|} + \sum_{i=1}^{N-1} \int \frac{\phi_i^* \phi_i}{|r - r_i|} d\tau \qquad (6)$$

In this equation, the first term describes the electrostatic attraction between $K$ nuclei and the outgoing electron, while the second term corresponds to the electrostatic repulsion between the outgoing electron and the remaining $N - 1$ electrons in their molecular orbitals ($\phi_i$) of the dianion. Note that the polarization from the excess electron and the correlation between the excess electron and the residue core are not included.

In this work, we introduce another approximation, the frozen anion-orbital static approximation distinguished from the above approximation by one electron being taken out of the highest occupied orbital of the dianion. In this approximation, we add one extra electron to the lowest unoccupied molecular orbital of the anion in which all of the occupied orbitals are frozen. This approach should better describe the interaction as the outgoing electron moves away from the remaining anion. Hence, the electrostatic potential is obtained by replacing $\phi_i$ in eq 6 by the frozen molecular orbitals of the anion. This approximation provides the long-range interaction tail which may be used to calculate the magnitude of the difference from the frozen dianion-orbital static approximation.

Figure 5 gives the estimated Hartree−Fock repulsive Coulomb barrier curves along the molecular axis $\hat{Z}$ (thick dashed lines) and its vertical axis $\hat{Y}$ (thick solid lines) for structures A, B, C, D, and E of the $BeC_4$ dianions at their equilibrium geometries. For isomer A, we compared the RCB using two approximations: the frozen dianion-orbital static approximation in A and the frozen anion-orbital static approximation in A*. In these cases, the two approximations are indistinguishable as the distance is larger than 20 Å. Thus, for other structures, we present only the results of the frozen dianion-orbital static approximation. The obtained RCBs for all of the structures are anisotropic in the ($Y-Z$) plane.

The above estimated repulsive Coulomb potentials were used to calculate the lifetime of the dianion in the framework of the WKB theory. The WKB lifetime (in atomic units) is given by

$$\tau = \frac{2d}{T_r \nu_{\text{inc}}} \qquad (7)$$

where $T_r = 4/(2f + 1/(2f))^2$ [28,29] is the transmission coefficient with $f = e^{\int_{r_1}^{r_2} \sqrt{2|E-V(r)|} dr}$, $E$ is the tunneling energy corresponding to electron velocity $\nu_{\text{inc}}$, and $V(r)$ is the frozen electrostatic potential obtained from ab initio calculations. $r_1$, $r_2$ are the small and large classical turning points, and $d$ is the effective length of the motion of the tunneling electron inside the potential well, which equals $r_1$ minus the size of the nuclear core. Note that the transmission coefficient of a one-dimensional barrier, $T_r = 1/f^2$, is suitable only for a high and broad barrier, that is, $f \gg 1$. Considering the large changes of the lifetimes in the present calculations from $10^{-2}$ to $10^{-15}$s, we choose a more general version of $T_r = 4/(2f + 1/(2f))^2$, in which $f$ is in $[0,\infty]$ for an arbitrary one-dimensional barrier.[29]

In the present calculation, the electron tunneling energy is estimated in two ways: as the negative value of the vertical electron detachment energy and as the adiabatic electron detachment energy. They are defined as follows:

$$E_{\text{vertical}} = E(\text{I}^-)|_{\text{f}} - E(\text{I}^{2-})|_{\text{opt}} \qquad (8)$$

$$E_{\text{adiabatic}} = E(\text{I}^-)|_{\text{opt,I}^{2-}} - E(\text{I}^{2-})|_{\text{opt}} \qquad (9)$$

where $E$(I) is the energy of a given isomer I, opt stands for optimized energy, $E(\text{I}^{2-})|_{\text{f}}$ corresponds to a single point energy calculated with frozen orbitals of the dianion $\text{I}^{2-}$, and $E(\text{I}^-)_{\text{opt,I}^{2-}}$ is the energy optimized starting from the equilibrium geometry of $\text{I}^{2-}$.

Table 2 provides lifetimes given by the HF calculations. Structure B is definitely an electron autodetachment (see insert B in Figure 5). Structure D has the largest time period of 0.1−0.4 ns. For structures A and C, the lifetimes along the $Y$ axis are smaller by a factor of 100 than those along the $Z$ axis. This shows that starting at the equilibrium geometry of the dianion, the electron tunneling takes place along the $Y$ axis.

To demonstrate the influence of the molecular dissociation on the electron tunneling, in Figure 6 we show two-dimensional pictures of the RCB for isomer A as a function of the dissociation path at the equilibrium point $R_{\text{dis}} = R_{\text{eq}} = 1.6462$ Å, at $R_{\text{dis}} = 3$ Å, and at $R_{\text{dis}} = 6$ Å. Obviously, the electron tunneling occurs at $R_{\text{dis}} > R_{\text{eq}}$ along a curved path between the $Y$ and the $Z$ axes. In Table 3, we list the lifetime values at $R_{\text{dis}} = 3$ Å along the $Y$ and $Z$ axes for all of the isomers. Our numerical calculations indicate that the dissociation of the molecule will accelerate the electron tunneling.

Comparing Tables 3 and 4, we note that the tunneling energy values from both the vertical and the adiabatic estimations[18] increase as $R_{\text{dis}}$ increases. As the tunneling energy becomes higher than the barrier maximum, autodetachment occurs. In

(28) Shi, Q.; Kais, S. *Mol. Phys.* **2002**, *100*, 475.
(29) Merzbacher, E. *Quantum Mechanics*; John Wiley & Sons: New York, 1961; p 126.

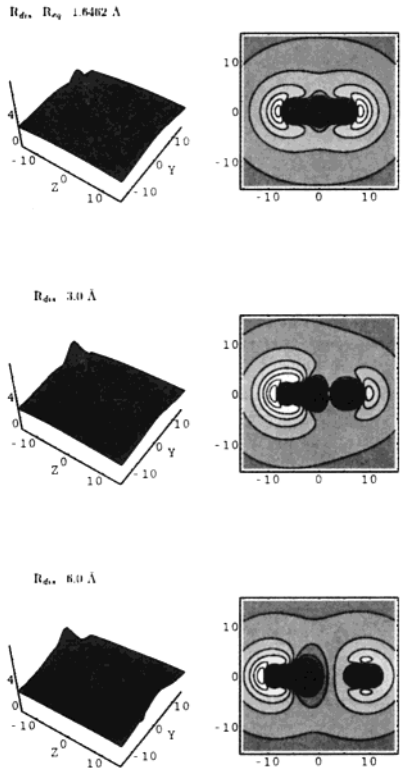

***Figure 6.*** Two-dimensional surfaces of the repulsive Coulomb barrier (eV) of isomer A, calculated using the frozen dianion-orbital static approximation along the dissociation path at its equilibrium point $R_{dis} = R_{eq} = 1.64622$ Å and two points along an energetically favorable dissociation pathway, $R_{dis} = 3$ and 6 Å. Here $Z$ is the molecular axis (Å), $Y$ is the vertical axis (Å), and $R_{dis}$ is the separation distance between the two fragments, $C_2^-$ and Be $C_2^-$. Contour lines projected in the $(Y-Z)$ plane for several heights of the barrier are also shown.

***Table 3.*** Estimated Lifetimes of Different Geometric Configurations at Their Equilibrium Points[a]

| | lifetime (s) at $R_{eq}$ | | | | | |
|---|---|---|---|---|---|---|
| | symmetrical | | | nonsymmetrical | | |
| structure | energy (eV) V/A | $RCB_Y$ | $RCB_Z$ | energy (eV) V/A | $RCB_Y$ | $RCB_Z$ |
| A | −0.2501 | ∞ | ∞ | 1.2495 | 9.20(−13) | 1.84(−11) |
| | −0.2389 | ∞ | ∞ | 1.3192 | 4.99(−13) | 1.10(−11) |
| A* | −0.2251 | ∞ | ∞ | 1.3871 | 1.06(−12) | 1.74(−14) |
| | −0.2389 | ∞ | ∞ | 1.3192 | 1.82(−12) | 2.62(−14) |
| B | | | | 7.7541 | AD[b] | AD |
| | | | | 7.8696 | AD | AD |
| C | | | | 2.9791 | 3.47(−15) | 1.53(−13) |
| | | | | 3.0866 | 2.74(−15) | 1.20(−13) |
| D | | | | 0.8600 | 3.91(−10) | 1.33(−10) |
| | | | | 0.9574 | 9.83(−11) | 3.93(−11) |
| E | 0.6737 | 3.20(−08) | 1.44(−08) | 1.3568 | 5.17(−12) | 3.35(−12) |
| | 0.7383 | 8.62(−09) | 4.03(−09) | 1.4955 | 1.90(−12) | 1.32(−12) |

[a] For each structure, there are two entry lines corresponding to the estimated electron tunneling energies which are the negative values of the vertical (V) and adiabatic (A) electron detachment energies of the dianion. An entry of the form 9.20(−13) means $9.20 \times 10^{-13}$. [b] AD: autodetachment.

Figure 7, we examine the variation of the barrier maximum $V_{RCB}^{max}$ (along the $Y$ axis) with $R_{dis}$. The crossing point $R_{dis}^c = 3.25$ Å is the point where the tunneling energy from the vertical calculation is equal to the barrier maximum. It is interesting to note that the electrostatic barrier peak is an oscillating function and goes down slowly as $R_{dis}$ increases.

There are two additional factors which absolutely increase the HF lifetimes in either orientation. First, we approximate the

***Table 4.*** Estimated Lifetimes of Different Geometric Configurations (at the Dissociation Point $R_{dis} = 3$ Å) of the Be $C_4^{2-}$ Dianion[a]

| | lifetime (s) at $R_{dis} = 3$ Å | | |
|---|---|---|---|
| | nonsymmetrical | | |
| structure | energy (eV) | $RCB_Y$ | $RCB_Z$ |
| A | 2.2617 | 1.38(−15) | 2.79(−14) |
| | 2.2836 | 1.31(−15) | 2.65(−14) |
| B | | AD[b] | AD |
| | | AD | AD |
| C | 5.4414 | AD | 1.15(−15) |
| | 5.5498 | AD | 1.23(−15) |
| D | 2.6471 | 1.25(−15) | 1.98(−14) |
| | 2.6855 | 1.15(−15) | 1.83(−14) |
| E | 2.4162 | 4.56(−15) | 7.32(−14) |
| | 2.4859 | 3.64(−15) | 5.97(−14) |

[a] As in the previous table, for each structure, there are two entry lines corresponding to the estimated electron tunneling energies which are the negative values of the vertical (V) and adiabatic (A) electron detachment energies of the dianion. An entry of the form 1.38(−15) means $1.38 \times 10^{-15}$. [b] AD: autodetachment.

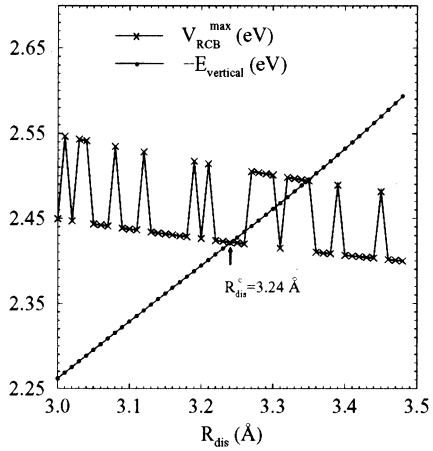


***Figure 7.*** Crossing between the maximum of the repulsive Coulomb barrier (eV) and the negative value of the vertical electron detachment energy $-E_{vertical}$, both of which are calculated at the Hartree−Fock level as a function of $R_{dis}$ (Å) for the $BeC_4^{2-}$ dianion. $R_{dis}$ is the separation distance between the two fragments, $C_2^-$ and $BeC_2^-$.

tunneling along a one-dimensional axis, neglecting the anisotropy of the two-dimensional potential, and, second, the HF tunneling energy is overestimated. Including electron correlations at the CISD level of theory for isomer A lowers the tunneling energy from about +1.3 eV down to about +0.3 eV (as shown in Figure 8). The CISD calculations give a lifetime of $4.45 \times 10^{+1}$ s (using the vertical approximation) and $5.56 \times 10^{-3}$ s (using the adiabatic approximation) along the $Y$ axis and $1.04 \times 10^{+2}$ s and $1.56 \times 10^{-2}$ s along the $Z$ axis, respectively. Hence, an approximate low limit of lifetime of $BeC_4^{2-}$ is about 5.6 ms. This lower limit is in agreement with the experimental results in which the $BeC_4^{2-}$ dianion is supposed to live markedly longer than 5 $\mu$s.[9] However, these results are only an "approximation" of the full two-dimensional tunneling calculations. A more accurate description of the tunneling, using multidimensional tunneling methods,[30−32] is still needed.

(30) Truhlar, D. G.; Garrett, B. C.; Klippenstein, S. J. *J. Phys. Chem.* **1996**, *100*, 12771.
(31) Fernandez-Ramos, A.; Truhlar, D. G.; Corchado, J. C.; Espinosa-Garcia, J. *J. Phys. Chem. A* **2002**, *106*, 4957.
(32) Pu, J.; Corchado, J. C.; Truhlar, D. G. *J. Chem. Phys.* **2001**, *115*, 6266.

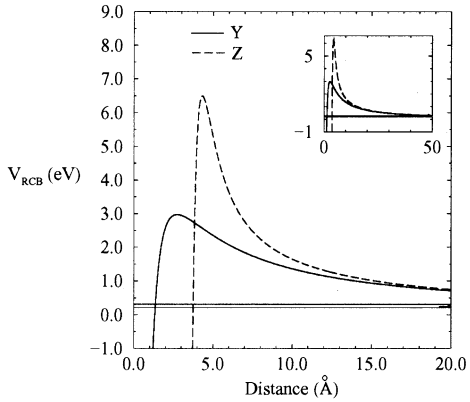


***Figure 8.*** One-dimensional cuts through the repulsive Coulomb barrier along the molecular axis $\hat{Z}$ (thick dashed lines) and its vertical axis $\hat{Y}$ (thick solid lines) for the geometric configuration A of $BeC_4$ dianions. The repulsive Coulomb barrier has been calculated using the frozen dianion-orbital static approximation at the level of configuration interaction with single plus double excitations. The thin solid lines are for the two estimations for the electron tunneling energy from the adiabatic electron detachment energy (up) and the vertical electron detachment energy (down).

## IV. Summary and Conclusions

We have examined five possible geometrically stable isomers of the $BeC_4^{2-}$ dianion. Among all of the possible isomers, we have found that isomer A, $C_2^-BeC_2^-$, has the lowest dianion energy and is stable with respect to fragmentation, but metastable with respect to electron detachment. This finding is in complete agreement with the previous work of Dreuw and Cederbaum.[18] All of the molecular geometries of $BeC_4$ isomers were optimized at the Hartree−Fock level with 6-311+G(d) basis set; this basis set seems sufficient to describe the characteristics of the examined isomers of $BeC_4$. The effect of electron correlation on the energetics of the optimized geometries was considered by calculations at the configuration interaction with single plus double excitations (CISD) and MP2. Our CISD results for the optimized energies at the equilibrium for $C_2BeC_2^{2-}$ were in complete agreement with the CCSD results.

We examined the Coulomb explosive images of the Klein and Middleton experiment[9] and showed how they might be related to our optimized structures. We found that the optimized structures for $BeC_4$ and $BeC_4^-$ are planar, but for the $BeC_4^{2-}$ dianion it is similar to isomer C. Because isomers C, D, and E are very close in energy, one can consider the possible motions of the tight C−C bonds relative to the Be atom to form the most stable form, which is isomer A. Thus, the intermediate images of the planar structures are consistent with our optimized structures.

The electron tunneling through the RCB was considered along the dissociation path to obtain $C_2^-$ plus $BeC_2^-$. We obtained the two-dimensional RCB using two approximations: the frozen dianion-orbital static approximation and the frozen anion-orbital static approximation. We used the RCB to estimate the lifetime of the metastable $BeC_4^{2-}$ dianion. In the framework of the WKB theory, the lifetime of the metastable $C_2^-BeC_2^-$ dianion was estimated to be about 5 ms. This lower limit is in agreement with the experimental results in which the $BeC_4^{2-}$ dianion is supposed to live much longer than 5 $\mu$s.[9]

Along the dissociation path, we note that the tunneling energy values from both the vertical and the adiabatic estimations increase as $R_{dis}$ increases. As the tunneling energy becomes higher than the barrier maximum, autodetachment occurs. We estimated the crossing point to be $R_{dis}^c = 3.25$ Å. At this point, the vertical electron detachment energy is equal to the barrier maximum. We would like to acknowledge the financial support of the NSF and ACS.

JA020116Q